Distribution of glial fibrillary acidic protein-immunopositive structures in the brain of the red-eared freshwater turtle (*Pseudemys scripta elegans*)

M. Kálmán, Á. Kiss, K. Majorossy

1st Department of Anatomy, Semmelweis University of Medicine, Budapest, H-1450 Hungary

Abstract. The distribution of glial fibrillary acidic protein (GFAP)-immunoreactivity is described in serial Vibratome sections of the turtle brain. The results are discussed in relation to our previous studies of rat and chicken brains. In the turtle brain, the distribution of GFAP-positive elements is rather evenly abundant as compared to that observed in the chicken and rat. The GFAP-positive structures are fibers of different length and orientation, but the stellate cells are not GFAP-positive. The basic systems is the radial ependymoglia, directed from the ventricles toward the outer surface of the brain. This system also contains some transverse and randomly oriented fibers. The cell bodies are not usually GFAP-positive. The large brain tracts could be recognized by their weak immunostaining, but gray matter nuclei could not be identified on the basis of immunostaining against GFAP. The layers of the optic tectum could be distinguished, as well as the gray and white matter of brain stem and spinal cord and the molecular and granular layers of the cerebellum. In the cerebellum, a fiber system resembling the Bergmann-fibers, a strong midline raphe and coarse transverse fibers could be observed. These latter fibers have no equivalent in other cerebella. Their perikarya proved also to be GFAP-positive, and seemed to be dividing in the adult turtle brain. We conclude that the appearance of GFAP-positive stellate cells had a great importance in the evolution of avian and mammalian brains strengthening the thicker brain walls and assisting in the formation of local differences of GFAP-immunoreactivity in different brain areas.

Key words: Glial fibrillary acidic protein – Glia – Turtle brain

Introduction

Glial fibrillary acidic protein (GFAP), the characteristic cytoskeletal protein of astroglia, can be found not only in mammals but also in birds, reptiles and fishes. In each

Correspondence to: M. Kálmán

group, the GFAP has a cross-reactivity to the anti-mammalian GFAP antibodies (Dahl and Bignami 1973; Dahl et al. 1985; Onteniente et al. 1983).

The distribution of GFAP immunopositivity has been described in a lizard species *(Gallotia galloti)* as a representative of reptiles (Monzon-Mayor et al. 1990; Yanes et al. 1990). The class of reptiles is, however, far less homogenous than that of birds and mammals. The reptilian phylogenesis proceeded along very divergent lines, and as the majority of reptiles had become extinct by the end of the Mesozoic era, the orders that survived are rather separate side-branches of the phylogenetic tree. In some structural details (temporal opening of skull, diaphragm, pulmonary circulation) their living or fossil groups show a closer relationship to the birds or mammals than to each other. Of the living reptiles, the turtles (Chelonia) seem to be most closely related to the common ancestors of reptiles (Cotylosauria), and they have changed little from the Triassic period (Romer 1959, 1972). It is also widely accepted that the turtle brain may have preserved the greatest number of features in common with the brain of the supposed reptile ancestors of mammals (see Connors and Krigstein 1986; Davydova and Goncharova 1979; Powers and Reiner 1980; Reiner 1991; Riss et al. 1969 for reviews).

A Golgi study of turtle glia has been made (Stensaans and Stensaans 1968), and the immunohistochemical cross-reactivity between mammalian and testudian GFAP has been demonstrated in a series of publications (Dahl and Bignami 1973; Dahl et al. 1985; Onteniente et al. 1983), while some investigations of the telencephalic glia have been reported (Kriegstein et al. 1986), but no comprehensive mapping has been published. We present here a systematic description of the distribution of GFAP-immunopositive elements in the red-eared freshwater turtle *(Pseudemys scripta elegans)*.

Materials and methods

Four young adult red-eared freshwater turtles *(Pseudemys scripta elegans)* of either sex and approximately 300 g weight were anes

thetized with hypodermic injections of sodium pentobarbital (37 mg/kg body weight) and then immersed in an ice-cold water bath for 60 min. The plastron was then cut away and the animals were perfused transcardially with 0.9% NaCl (6° C) and then with 500 ml 4% paraformaldehyde in phosphate buffer (0.1 M, pH 7.4). The brains were dissected and postfixed in the same fixative for 48 h at 4° C. After a rinse in phosphate buffer, the brains were embedded in agar, and then 80-μm-thick serial sections were cut in the coronal plane by a Vibroslice vibrating microtome.

After an overnight wash in phosphate buffer, the sections were pre-treated with 3% H_2O_2 (5 min) and then incubated in 20% normal goat serum for 1.5 h at room temperature to suppress background staining. These and the following steps all included a rinse with phosphate buffer between the changes of immune reagents. The mouse monoclonal antibody was produced by Boehringer (Mannheim) against porcine GFAP (for references, see Debus et al. 1983). The anti-GFAP antibody was applied at a dilution of 1:100 in phosphate buffer containing 0.5% Triton X–100 (the final concentration of antibodies was 200 ng/ml) for 40 h at 4° C. As a secondary antibody, biotinylated rabbit anti-mouse immunoglobulin was used, and then the sections were incubated in streptavidin-biotinylated horseradish peroxidase complex. Both reagents were purchased from Amersham, diluted 1:100 and applied for 1.5 h at room temperature. The immunocomplex was visualized by the diaminobenzidine reaction, 0.05% 3-3′-diaminobenzidine in 0.05 M TRIS-HCl buffer (pH 7.4) containing 0.01% H_2O_2, for 10 min at room temperature. No diaminobenzidine reaction product was found when the anti-GFAP antibody was omitted from the procedure.

For orientation, series of sections were collected and stained with cresyl violet according to Nissl. For mapping, the outlines of sections were drawn with a microscope slide projector, and the position of the respective microscopic fields was recorded on these templates. In the identification and the nomenclature of turtle brain structures we followed Ariens Kappers et al. (1960) and the turtle stereotaxic atlas of Powers and Reiner (1980).

Results

In the turtle brain the GFAP-immunopositive elements are long fibers forming dense textures almost everywhere (Fig. 1), but no GFAP-positive stellate cells can be found. The general pattern consists of thick fibers running from the ventricular system toward the brain surface, while finer secondary fibers cross and enmesh this system. At some places, among the latter, there are sinuous fibers ending in perikaryon-like intumescenses (Fig. 2). Neither surface-limiting nor perivascular glia can be distinguished. The outer surface of the brain is lined densely by the endings of straight glial fibers, while other fibers reach the blood vessels at different angles and weave around them a glial sheath (Figs. 3, 4) that is not always continuous.

In the rostral part of the telencephalon (Fig. 5) the GFAP-immunopositive fibers form coarse and wavy bundles at the ventricular surface. Coursing toward the pial surface, they branch in brush-like fashion and become thinner and less regularly arranged. As they reach the pial surface, the fibers converge again. In this way we can distinguish three zones in the telencephalic wall: rather well-organized deep and superficial zones and an irregular middle zone. In some places a "bushy" origin of fibers can be observed (Fig. 6). The olfactory tracts are separated by coarse bundles of GFAP-positive fibers,

while the tracts themselves contain fibers that are barely immunopositive (Fig. 7).

The less regular the ventricular contour becomes, by the bulging of the septum, the ventral striatum and the dorsal ventricular ridge (Fig. 8), the more complex is the glial pattern that can be found. In the dorsal and dorsomedial cortex, where the thickness does not change, the glial pattern remains similar to that described above, although the fibers starting from the ventricle are not so coarse. Above the septum, in the medial telencephalic wall, some fibers diverge obliquely from the fiber systems perpendicular to the pial or ventricular surfaces. These diverging fibers curve dorsalward from both sides of the telencephalic wall and cross in the middle, forming a mesh of X-pattern, and then they continue in parallel with the ventricular wall (Fig. 9). In the thickened parts (septum: Fig. 10, ventral striatum: Fig. 11) the deep zone of straight fibers thickens in correspondence with the protrusion of the wall into the ventricle. In the dorsal ventricular ridge (Fig. 12), the fibers are oriented from the convex ventricular surface toward the center of the ridge, where they form a bundle and run lateralward out of the ridge. At the corners of the ventricle, mainly between the ventral striatum and the dorsal ventricular ridge, the GFAP-immunopositive fibers are strongly curved and can almost be followed to the outer surface (Fig. 13). At the posterior part of the ventral striatum poorly immunostained areas indicate the position of the lateral forebrain bundle (Fig. 14). The loose fascicles of glial fibers are oriented in parallel with the nerve fibers (Fig. 15).

The most variegated distribution of GFAP-immunopositive elements can be found in the diencephalon (Fig. 16). The optic tract is demarcated by a thick plexus of glial fibers (Fig. 17). Inside the tract, we can see scattered coarse processes parallel with the optic fibers. The ventral part of the hypothalamus has a very dense fiber network (Fig. 18), while in the dorsal hypothalamus (Fig. 19), where we find a looser pattern, the basic fiber

---

Fig. 1. The basic glial pattern of the turtle brain. The system of radial fibers *(arrowheads)* is enmeshed by thinner fibers running in a different direction. × 250

**Fig. 2.** Sinuous fibers with perikaryon-like intumescences *(arrowheads)* × 200

Fig. 3. A blood vessel sectioned tangentially. The surrounding GFAP-positive fibers form endfeet in some places, while in others the glial sheath is not continuous *(arrow)*. In the thick section the tangential fibers can be seen to overlap the lumen. × 200

Fig. 4. GFAP-positive fibers winding around a blood vessel. × 250

Fig. 5. The wall of the olfactory ventricle. Three zones can be distinguished: rather well-organized inner and outer zones and an irregular middle zone *(im, om,* the inner and outer borders of the middle zone). Note the foot-plate and the characteristic division of the thick fibers *(arrow)* originating from the ventricle wall *(V)* b, blood vessel. × 150

Fig. 6. "Bushy" origin of fibers at the ventricular surface. × 250

Fig. 7. The olfactory tract. Coarse glial septa separate the nerve bundles, which can be seen as light areas. × 100
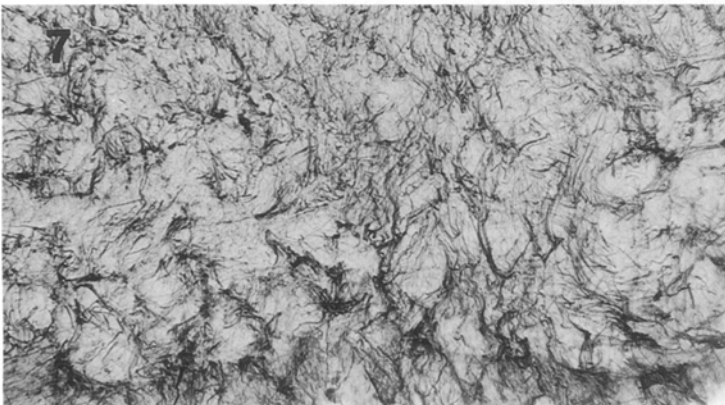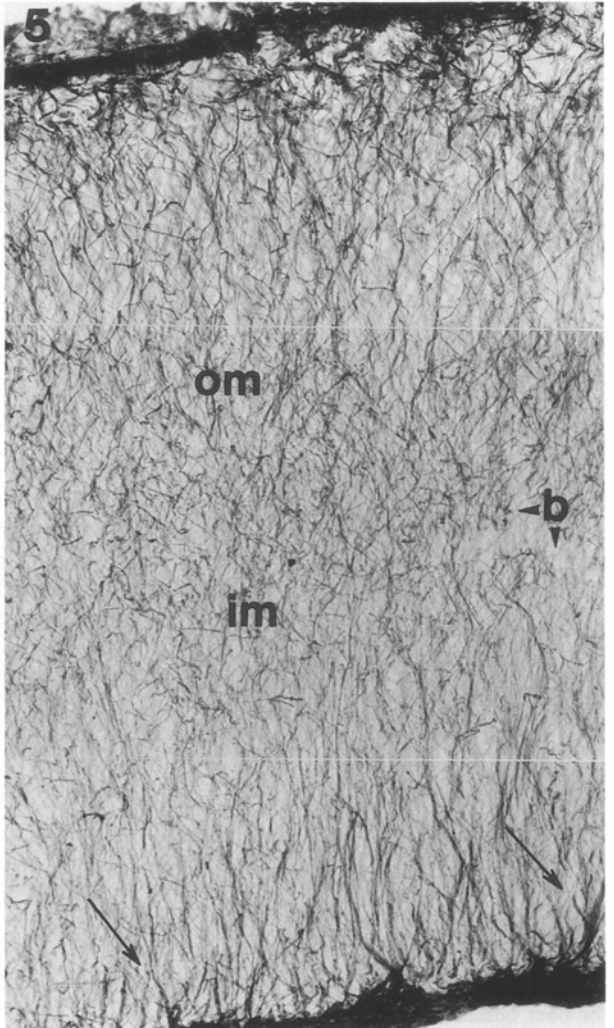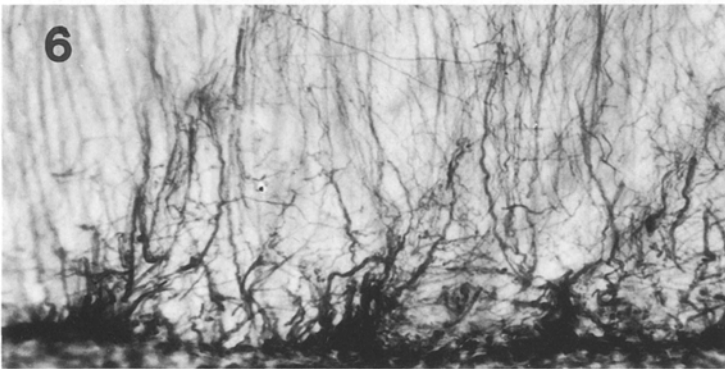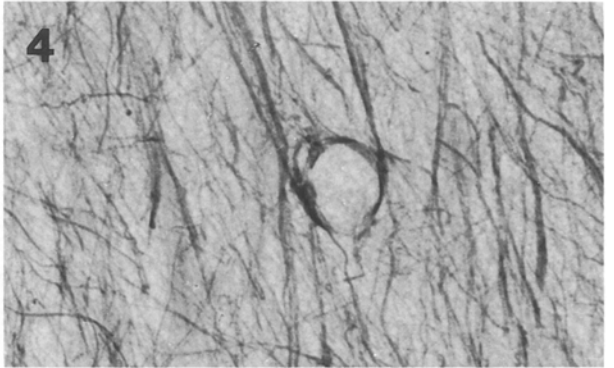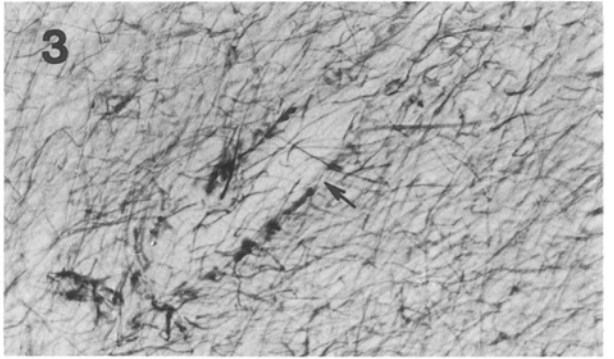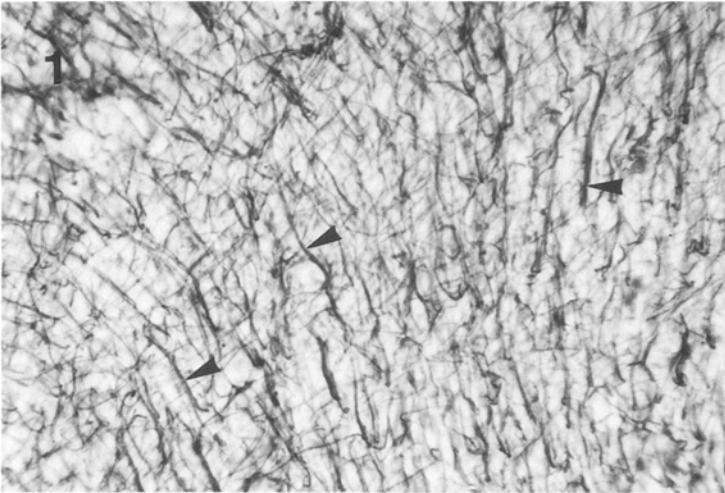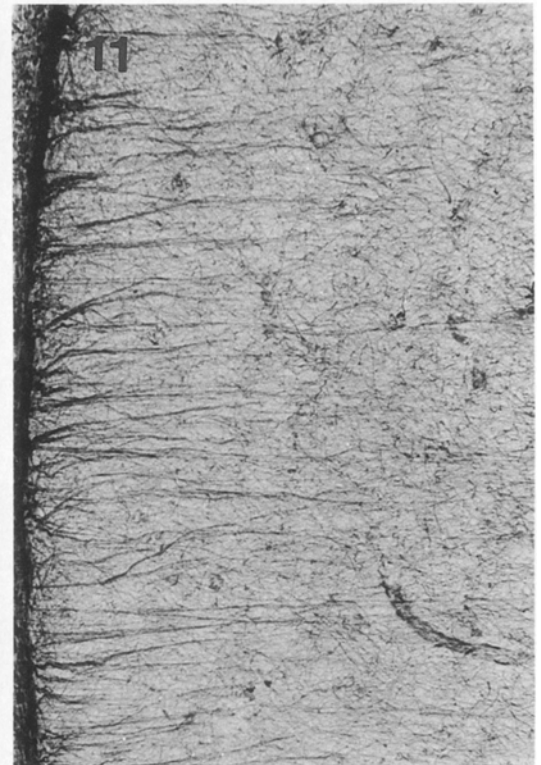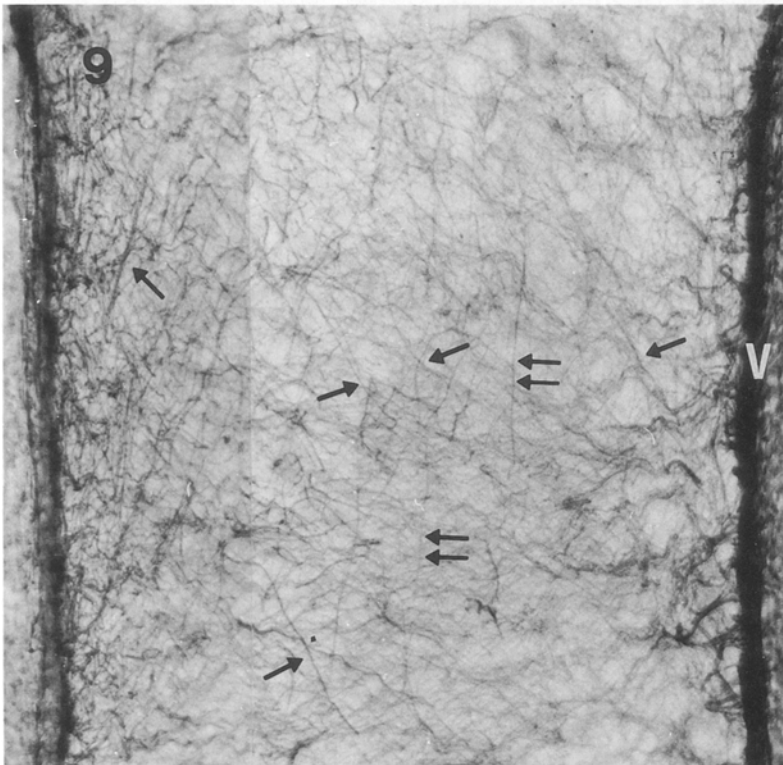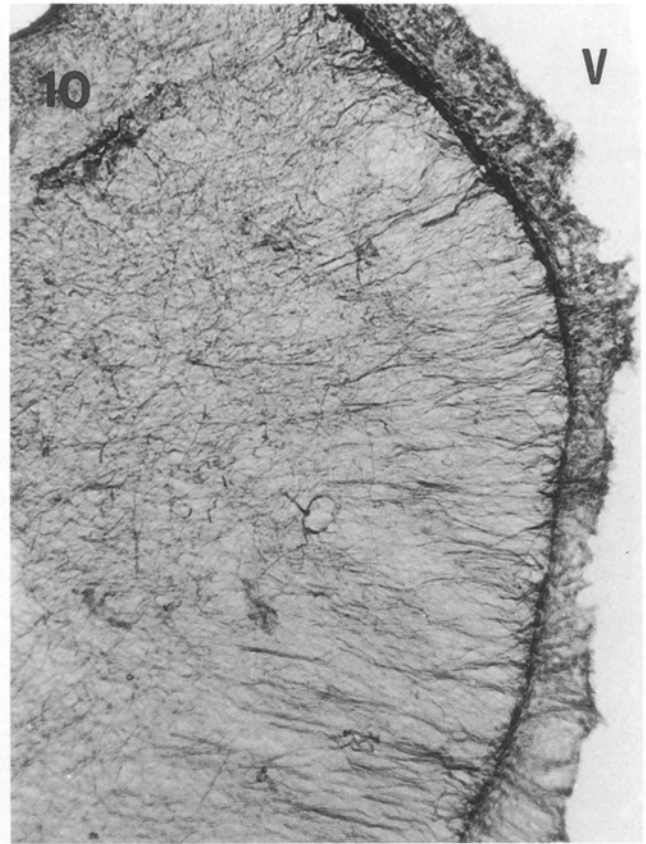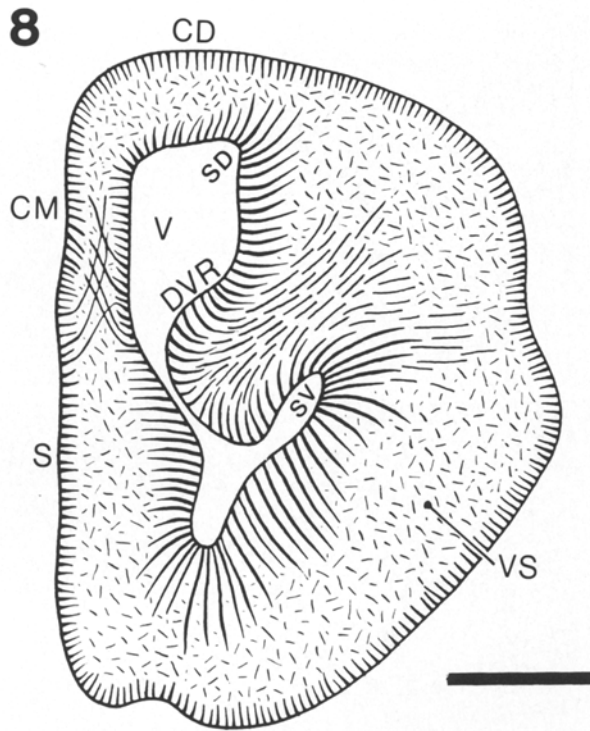
Fig. 8. Schematic drawing of the coronal section of the turtle forebrain in front of the optic chiasma, showing the distribution of GFAP-positive fibers. *V*, Ventricle; *CD*, and *CM*, dorsal and medial corticoid area (see Fig. 9); *S*, septum (Fig. 10); *VS*, ventral striatum (Fig. 11); *DVR*, dorsal ventricular ridge (Fig. 12); *SD*, and *SV*, dorsal and ventral sulcus of ventricle (Fig. 13). Note the supposed transformation of radial fibers into transverse fibers in CM, the fiber bundle oriented outward from *DVR*, and the long fibers at *SV*. *Bar* 1 mm

Fig. 9. The telencephalic wall above the septum (see *CM* in Fig. 8). Note the long fibers coming obliquely from both surfaces and crossing in the middle *(arrows)*. Some of them are almost parallel with the surface *(double arrows)*. *V*, Ventricular surface. × 150

Fig. 10. Septum. Note the long straight fibers. *V*, ventricle. × 100

Fig. 11. The ventral striatum. The fibers originating from the ventricle are longer, thinner, less densely arranged and less branching than in the thinner parts of the telencephalic wall (for comparison, see Fig. 5). × 100
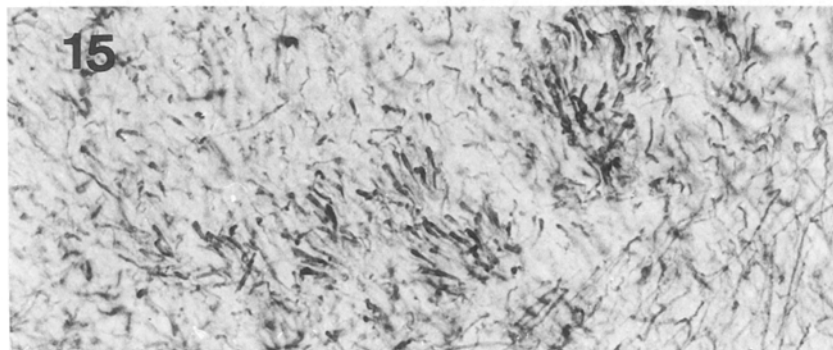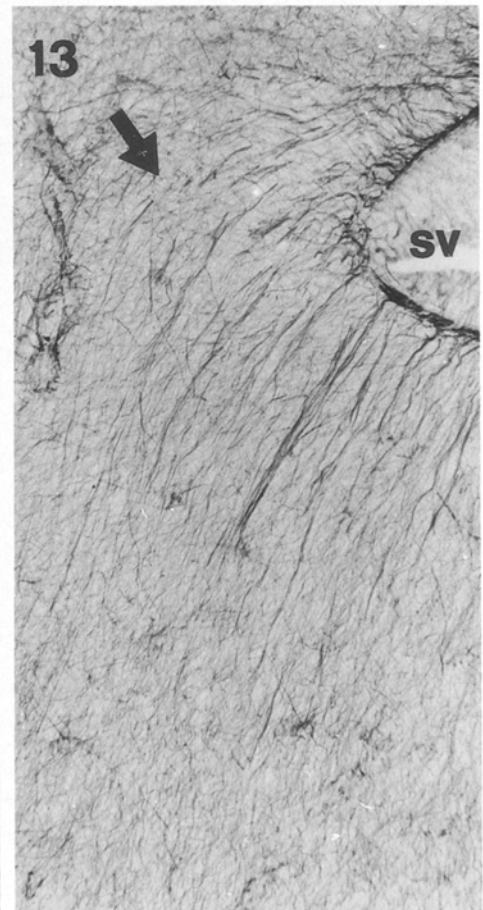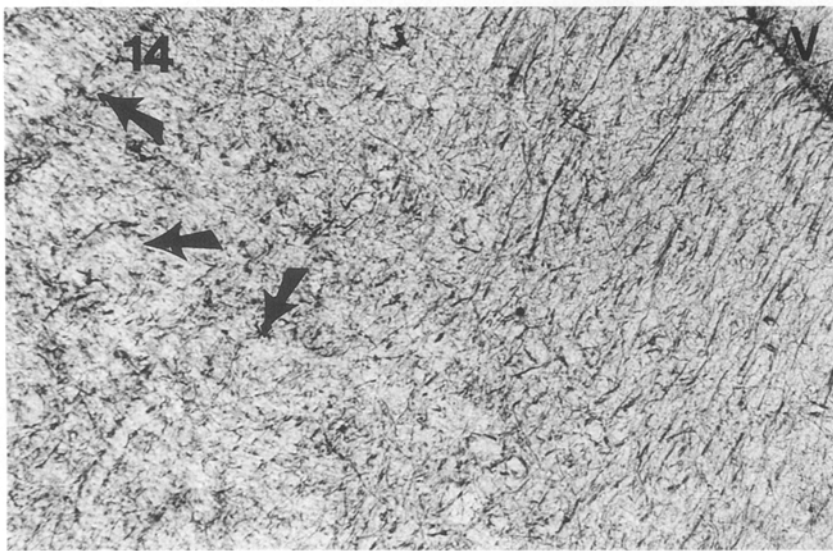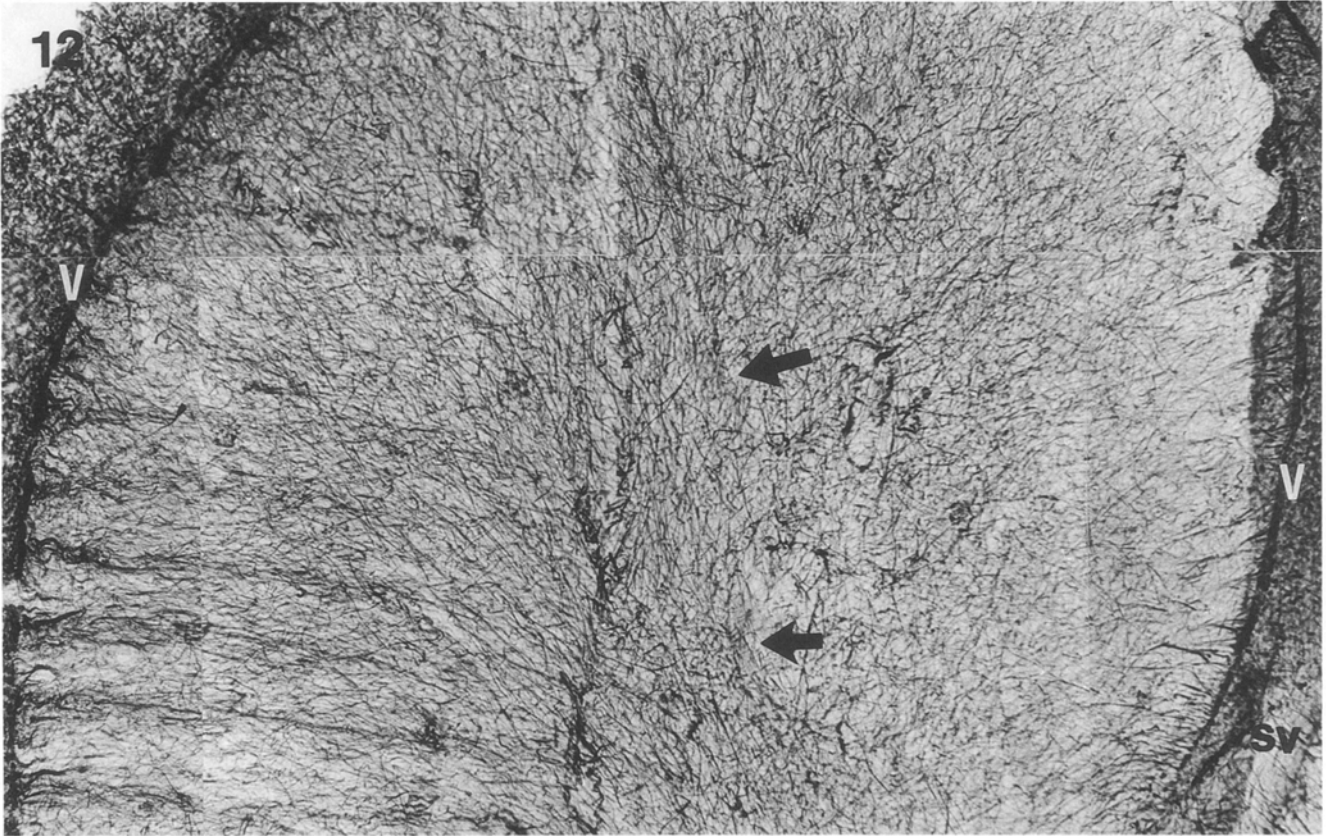
Fig. 12. The dorsal ventricular ridge. The fibers originating from the convex ventricular surface (*V*) gather into a bundle *(arrow)* in the middle of the ridge and then course outward. *SV*, ventral sulcus of ventricle. × 100

Fig. 13. The characteristic curvature of fibers *(arrow)* at the ventral sulcus (*sv*) of the ventricle (see *SV* in Fig. 8). × 200
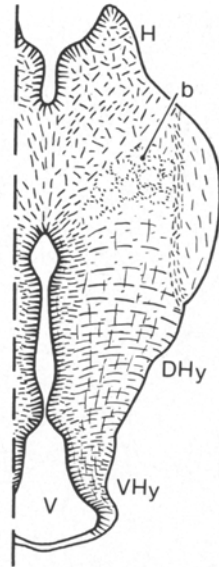
Fig. 14. The lateral forebrain bundle in the telencephalic wall at the level of the optic chiasma. The GFAP-poor areas *(arrows)* correspond to the groups of nerve fibers that are interspersed with groups of concomitant parallel glial fibers (see enlarged in Fig. 15). *V*, Ventricle. × 100
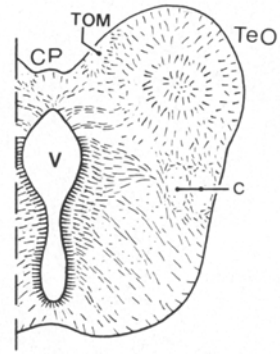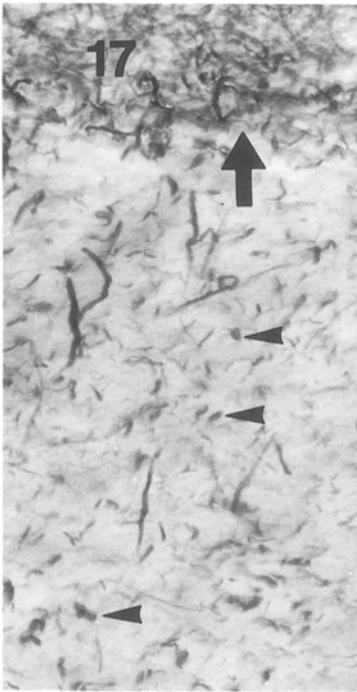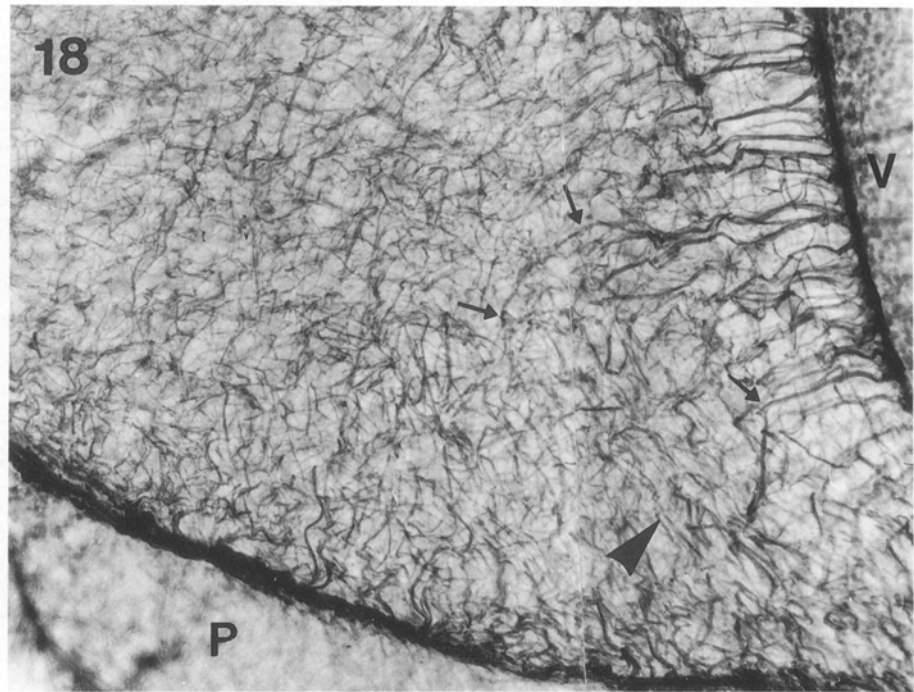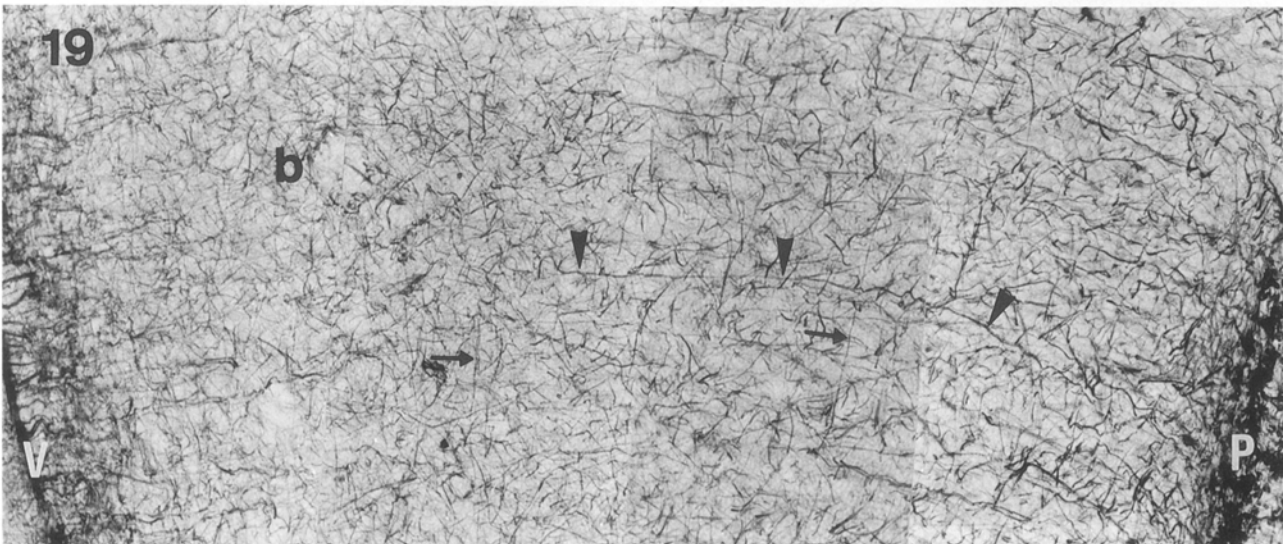
Fig. 15. Enlarged part of Fig. 14. × 250
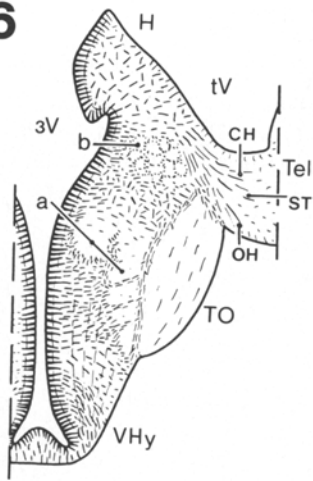
arrangement can be observed more readily. The thickest fibers can be traced from the ventricle to the pial surface, and as they touch both surfaces at a right angle, they form dorsally convex arches. The thinner the hypothalamic wall becomes ventrally, the stronger is the curvature of these fibers as they take a direction perpendicular to the pial surface (Fig. 18). Another system of fibers courses dorsalward from the bottom of the third ventricle (Figs. 18, 19). A condensation of fine fibers running in parallel with the ventricular surface (see also in Fig. 20, upper inset) forms a periventricular fiber system around the third ventricle.

The density of GFAP-immunopositive fibers clearly demarcates the area of the diencephalic grey matter (Fig. 20). The loose formations of the forebrain bundles can be recognized as pale, GFAP-poor spots intermingled with GFAP-rich ones, while the corticohabenular tracts and the stria terminalis can be traced by long GFAP-positive fibers. The optic tract shows the same structure as described above. In coronal section, the arrangement of GFAP-positive fibers can be observed more easily at this level, where the tract curves upward (Fig. 20, lower right inset), than rostrally near to the chiasma.

In the caudal part of the diencephalon (Fig. 16B, C) and in the mesencephalon (Fig. 21) the densely immunolabeled area of the grey matter follows the shape of the ventricle. The peripheral zone corresponding to the white matter has a less dense population of GFAP-positive fibers, except where strong fascicles from the grey matter intersect it periodically (Fig. 22). We can recognize the radiation of Meynert (Fig. 23), the tectothalamic tract and the medial longitudinal fascicle. The tracts of the posterior commissure, which have only a few

GFAP-containing glial fibers, form a light "keystone"-like area on the top of the third ventricle (Fig. 24). Radiating from here, these tracts can be followed as GFAP-poor strips around the upper part of the ventricle (Fig. 25). The lateral and medial marginal optic tracts (Fig. 26) also show a conspicuously weak immunoreactivity. The layers of the optic tectum can be distinguished clearly in GFAP-immunostained sections (Fig. 27). In the layers that contain mainly nerve fibers, the radial system of glial fibers is interspersed by GFAP-poor spots, while in the other layers the immunopositive elements are distributed rather evenly. The inferior colliculus has a dense irregular network of GFAP-immunopositive fibers (Fig. 28).

In the lower brain stem, the difference between the immunopositivity of grey and white matter is obvious (Fig. 29). The GFAP-immunopositive fibers form a very dense network in the grey matter, although the white matter also contains numerous coarse fibers. The raphe is intensively immunostained. The medial longitudinal fascicle, which is well circumscribed within the caudal part of the mesencephalon, seems to be mingled with the common white matter in the pons. The distribution of GFAP-immunopositivity follows a similar pattern in the closed part of the medulla and in the spinal cord (Fig. 30), but the structure of the white matter becomes more organized as the nerve fascicles are separated and ensheathed by the bundles of glial fibers (Fig. 31).

In the deeper part of cerebellum (Fig. 32), mainly around the ventricle, the distribution of GFAP-positive elements resembles the GFAP-pattern of the white matter tracts. In the midline a dense population of fibers forms a "pony-tail" ascending to the surface (Figs. 32, 33). The granular and molecular layers of the cortex can be clearly distinguished, both containing fibers oriented perpendicularly to the surface (Fig. 33), but the fiber system of the granular layer is rather coarse, while that of the molecular layer is finer, and does not seem to be a continuation of the former. Neither of the fiber systems is arranged evenly: stripes packed more densely alternate with looser zones rather irregularly.

The most striking structure however, is a system of fibers traversing the molecular layer (Fig. 32). In the midline they cross the "pony-tail" (Fig. 33), then laterally do not follow the curvature of the cerebellar surface, but keep their direction, so that at the lateral edge of the cerebellum they cross the surface-oriented fiber system at an acute angle (Fig. 32, inset). The cytoplasm of some perikarya also showed immunoreactivity, forming a ring around the immunonegative nucleus (Fig. 34). Perikarya with two nuclear "holes" (Fig. 35) and pairs of perikarya sending their processes in opposite directions can also be observed (Fig. 33), suggesting that cell division is taking place.

Fig. 16A–C. Schematic drawings of the distribution of GFAP-positive fibers in the different levels of the diencephalon. A is behind the anterior commissure, B is the middle part, C at the posterior commissure. The middle part of A is shown in a photomontage in Fig. 20. $V,3V$, Third ventricle; tV, telencephalic ventricle; H, habenula; TO, optic tract; Tel, the adjoining part of the telencephalon; VHy and DHy, ventral and dorsal parts of hypothalamus (Figs. 18 and 19, respectively); TeO, optic tectum (in tangential section at this level); CP, posterior commissure (see Fig. 24 and 25); a, medial forebrain bundle (medial dot) and the ventral peduncle of the lateral forebrain bundle (lateral dot); b, dorsal peduncle of lateral forebrain bundle; c, tectothalamic (medial dot) and lateral marginal optic (lateral dot) tracts; CH, corticohabenular tracts; ST, stria terminalis; OH, olfactohabenular tracts; TOM, medial marginal optic tract. Bar 1 mm

Fig. 17. The optic chiasma. The majority of glial fibers (arrowheads) can be seen in cross section i.e., they are parallel with the nerve fibers. Note the demarcating glial septum (large arrow). × 250

Fig. 18. The ventral part of the hypothalamus. Note the thick fibers (arrows) that originate from the ventricular wall (V) and curve toward the pial surface (P), and the group of ascending fibers (arrowhead). × 250

Fig. 19. The dorsal part of the hypothalamus. The fibers originating from the ventricular surface (V) can be followed (arrowheads) to the pial surface (P). The ascending fibers (arrows), having spread out, form a looser system here. B, Blood vessel. × 150

Discussion

The GFAP-immunoreactivity of the turtle brain proved to be intense, in accordance with preliminary data published by other authors (Dahl and Bignami 1973; Dahl
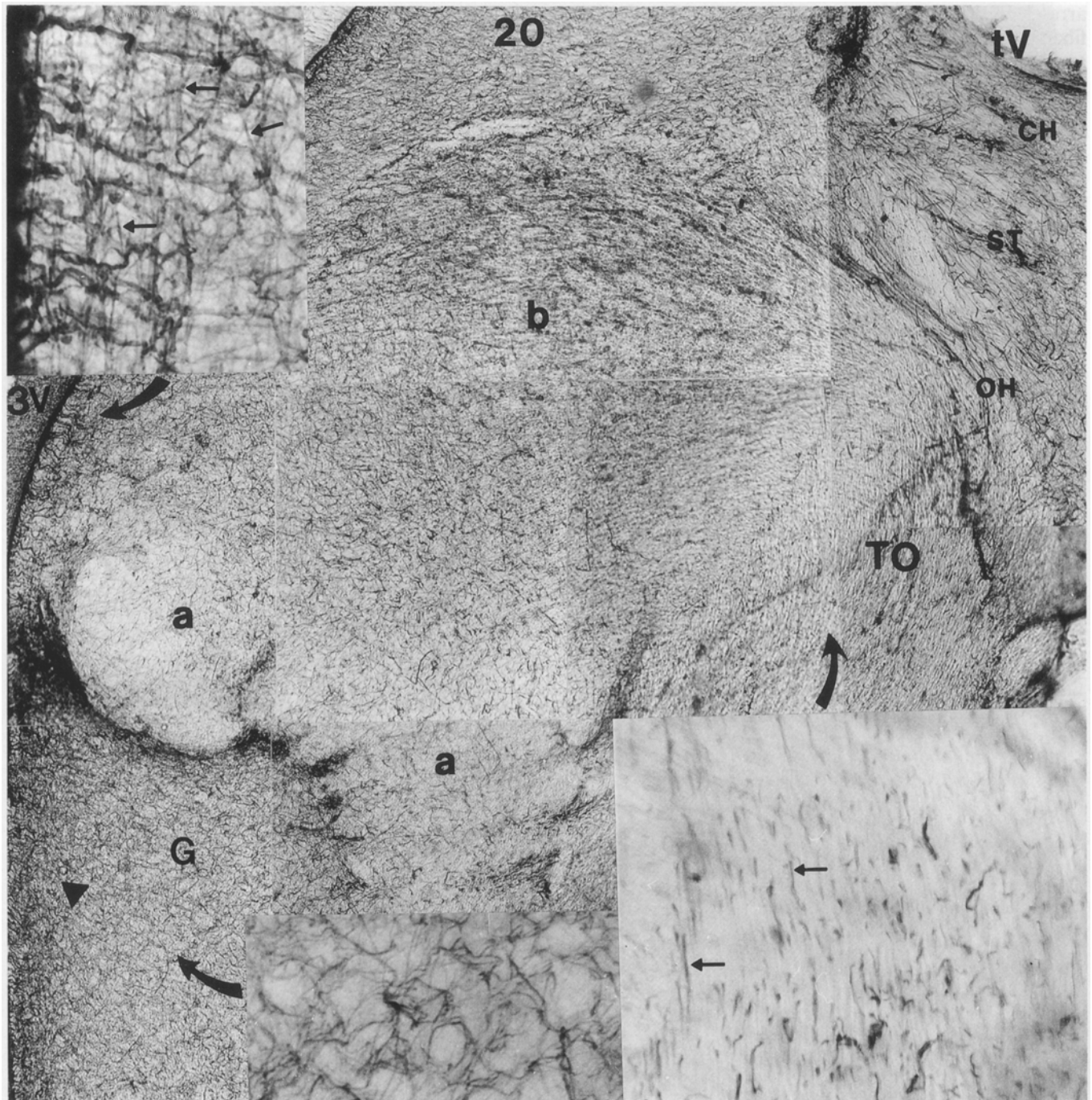
Fig. 20. The middle part of the coronal section shown in Fig. 16A. × 70 G, Periventricular gray matter. For the other abbreviations see Fig. 16. The arrangement of glial and nerve fibers in the dorsal peduncle of lateral forebrain bundle (*b*) is very similar to that shown in Fig. 15. *Upper inset:* the fine periventricular fibers *(arrows)* that enmesh the thick fibers originating from the third ventricle. × 300.

Lower right inset: a longitudinal section of the optic tract. Note the orientation of the glial fibers *(arrows)*. × 300. *Lower left inset:* an enlargement of an area (*black trigone* in the montage) where the fiber system is very dense and the spaces of neurons appear as light spots. × 500. *Curved arrows* show the areas enlarged in the insets

et al. 1985; Onteniente et al. 1983). GFAP-positive elements were more densely packed and much more evenly distributed than in the brains of mammals (rat: Hajós and Kálmán 1989; Kálmán and Hajós 1989; Zilles et al. 1991) or birds (chicken: Kálmán et al. 1993). There were no striking differences between the immunoreactivity of neighboring nuclei, by contrast to our earlier observa-

tions of the chicken (e.g., the ectostriatum versus the neostriatum, the paleostriatum primitivum versus the paleostriatum augmentatum) and the rat (e.g., the pallidum versus the striatum, the substantia nigra and interpeduncular nucleus versus the surrounding mesencephalic areas). In fact, no nuclei can be identified clearly in the GFAP-immunostained turtle brain.
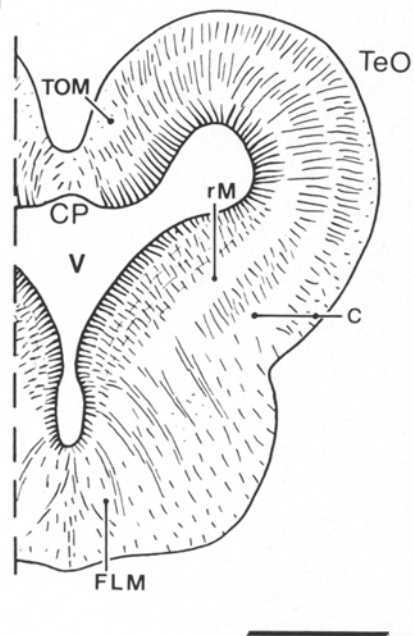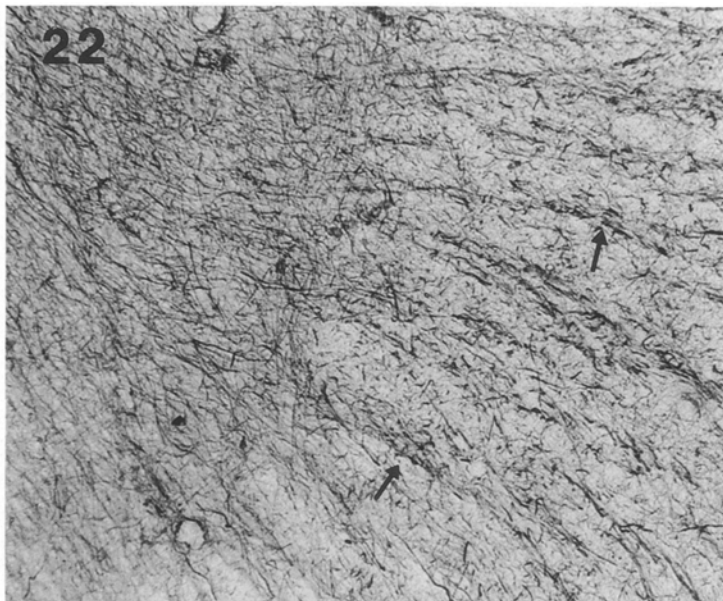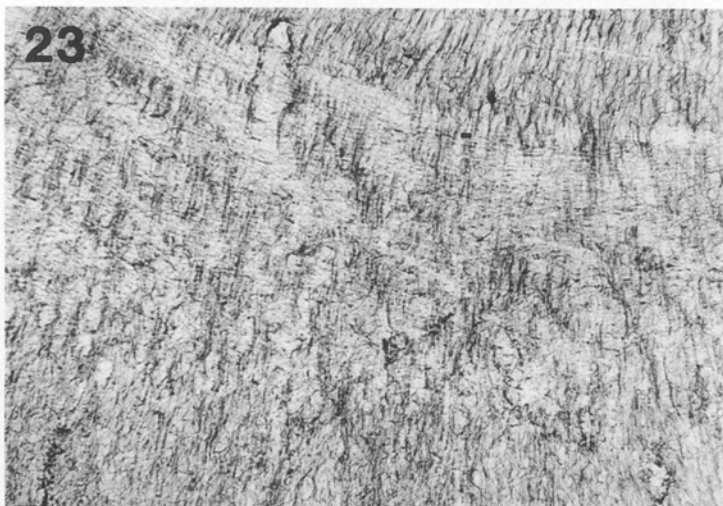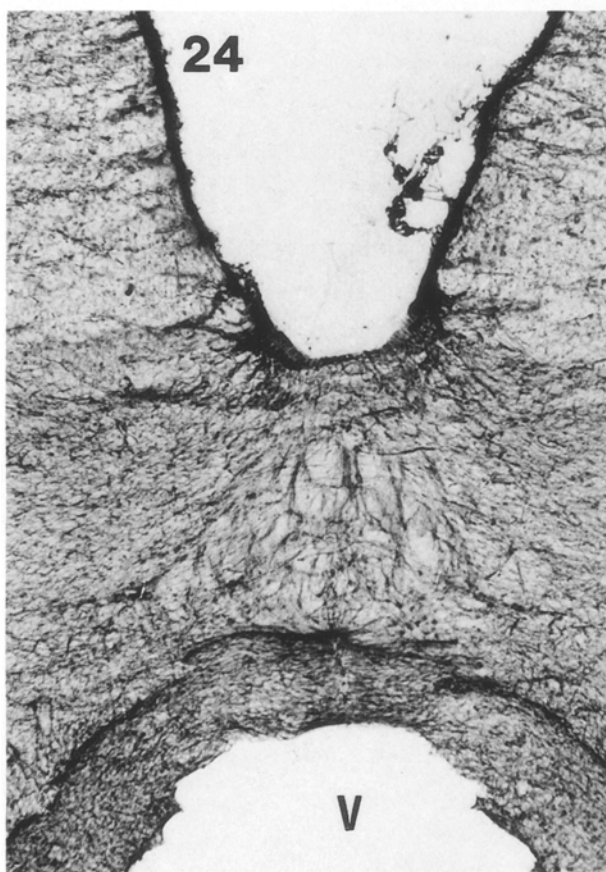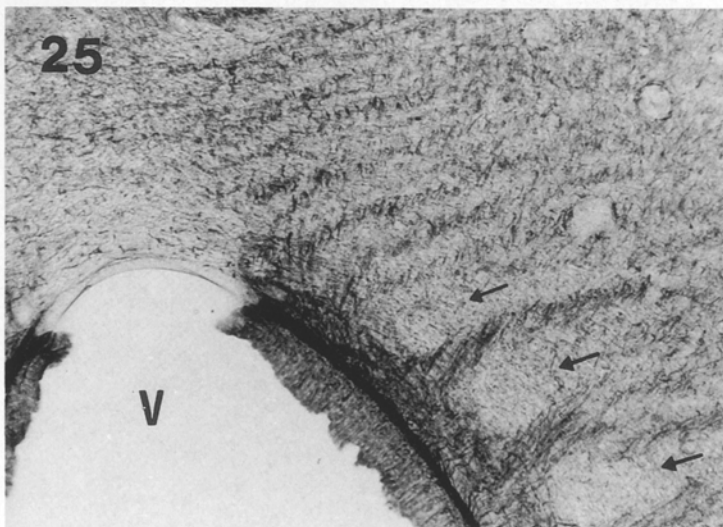
Fig. 21. Schematic drawing of the distribution of the GFAP-positive fibers in the mesencephalon. *V*, Ventricle; *CP*, posterior commissure (see Fig. 24); *TeO*, optic tectum (Fig. 27); *rM*, radiation of Meynert (Fig. 23); *TOM*, medial marginal optic tract (Fig. 26); *FLM*, medial longitudinal fascicle; *c*, the tectothalamic and lateral marginal optic tracts (*medial* and *lateral dots*, respectively). *Bar* 1 mm

Fig. 22. The border zone of the periventricular gray matter (*G*). Note the protruding bundles of glial fibers *(arrows)*. × 100

Fig. 23. The larger nerve tracts (here the radiation of Meynert) can be recognized as GFAP-poor strips interrupting the GFAP-positive fiber system. × 100

Fig. 24. The GFAP-poor tracts of the posterior commissure with separating glial fibers between them. *V*, Ventricle. × 100

Fig. 25. The radiation of commissural tracts around the upper part of the ventricle (*V*) (this level corresponds to that shown in Fig. 16C) intersperse the GFAP-positive fiber system *(arrows)*. × 100
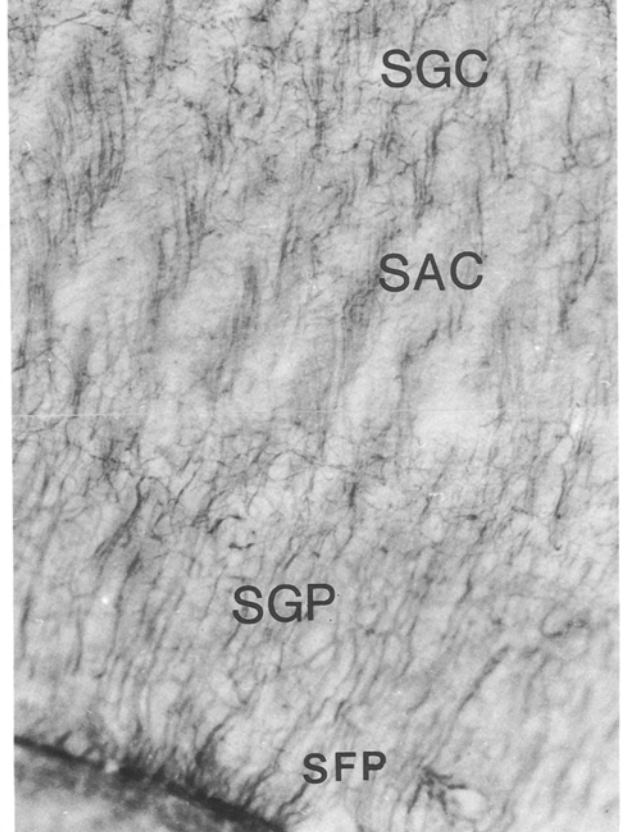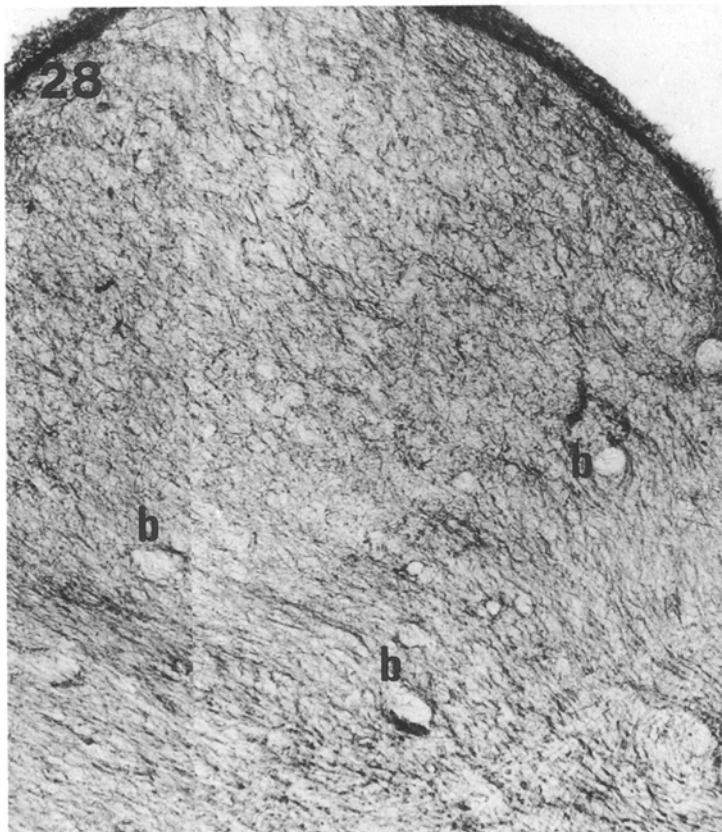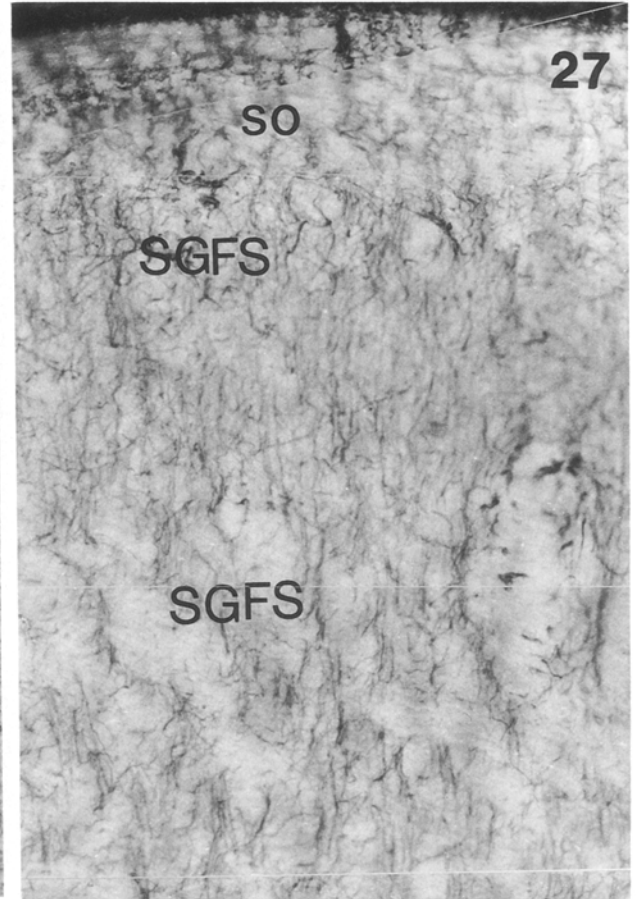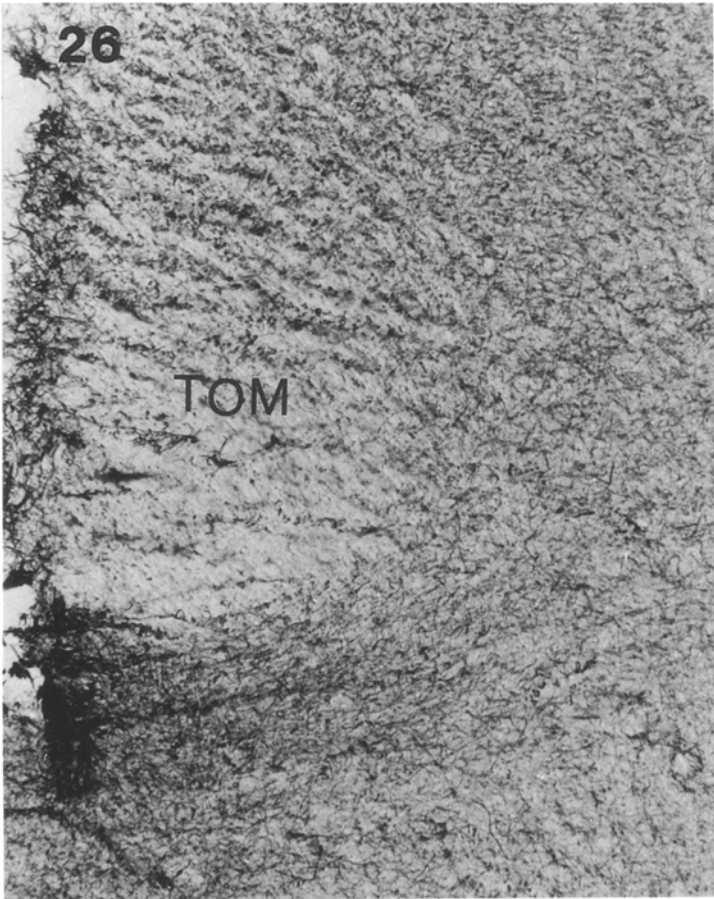
Fig. 26. The GFAP-poor area of the medial marginal optic tract (*TOM*). The surrounding radial tectal fibers can be seen in cross or oblique section in this plane. × 120

Fig. 27. The layers of the optic tectum. The GFAP-poor spots correspond to axon bundles. *SO, SFGS, SGC, SAC, SGP* and *SFP*, stratum opticum, fibrosum et griseum superficiale, griseum centrale, album centrale and fibrosum periventriculare, respectively. × 200

Fig. 28. The inferior colliculus. Note the dense fiber system. The small empty places correspond to neurons. *b*, Blood vessels. × 80

In accordance with the findings of Onteniente et al. (1983) we found no immunopositive stellate cells, although Stensaans and Stensaans (1968) have demonstrated astrocyte-like cells by Golgi impregnation in the turtle brain. Some GFAP-immunopositive stellate cells were observed in the brains of the snake (Onteniente et al. 1983) and lizard (Monzon-Mayor et al. 1990), i.e., in the phylogenetically "younger" reptiles, but the dominant GFAP-positive elements are long fibers in every reptilian brain.

The radial fiber system, which seems to originate from the ventricular surface and can be traced to the pial surface, is thought to be ependymoglia. Its GFAP-immunoreactivity in the turtle brain was debated earlier by Dahl and Bignami (1973), but has been documented by Onteniente et al. (1983) in the diencephalon and by Kriegstein et al. (1986) in the telencephalon. A similar fiber system was described by Yanes et al. (1990) as the primary glial system in the lizard. These fibers can safely be considered as equivalent to the embryonic radial glia of mammals (for review, see Hajós and Bascó 1984; Rakic 1981).

Where the original straight radial arrangement is modified, e.g., in the dorsal ventricular ridge, at the ventricular sulci and in the hypothalamus, this is probably the effect of the morphogenetic processes that have distorted the simple neural tube. A similar rearrangement of the simple original pattern can also be observed in the case of the remaining radial fibers of the chicken brain (Alvarez-Buylla et al. 1990; Kálmán et al. 1993a). The transverse fibers described by Kriegstein et al. (1986) in the turtle telencephalon are also most probably the continuations of the obliquely diverging fibers shown in Fig. 9.

Whether all the thin and irregular, "secondary" fibers are branches of the radial fibers or not, remains an unresolved problem. Usually they seem to be independent from the radial fibers and might belong to cell bodies showing no immunoreactivity against GFAP, except in some special cases, e.g., the transverse fibers of the cerebellum.

In the large tracts of the turtle brain the GFAP-immunostaining follows a similar tendency to that observed in mammals and birds (Hajós and Kálmán 1989; Kálmán et al. 1993a), i.e., the GFAP-immunopositive elements are coarse but rather scarce, so the tracts can be recognized as "light" areas. The strong glial demarcation of the optic and olfactory tracts cannot be observed in higher Vertebrates. The question whether the orientation of the GFAP-positive fibers along the nerve tracts is due to a former "guidance" function helping axonal
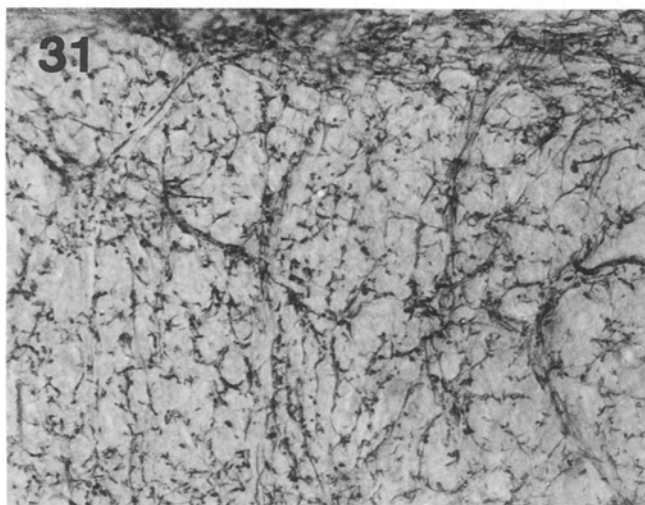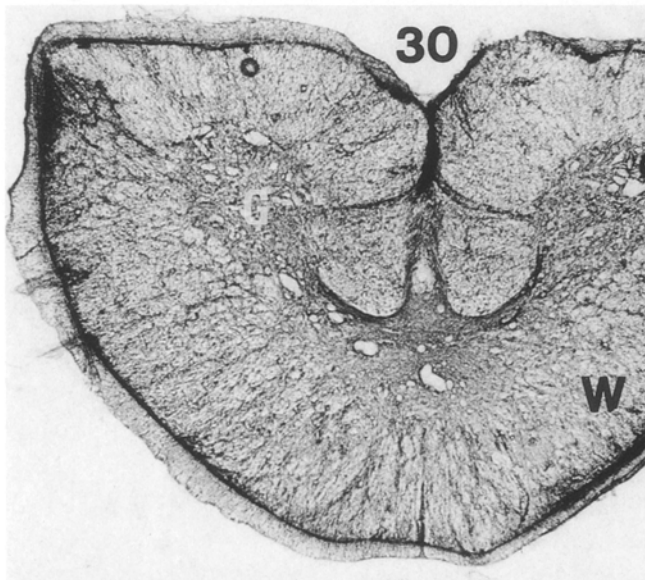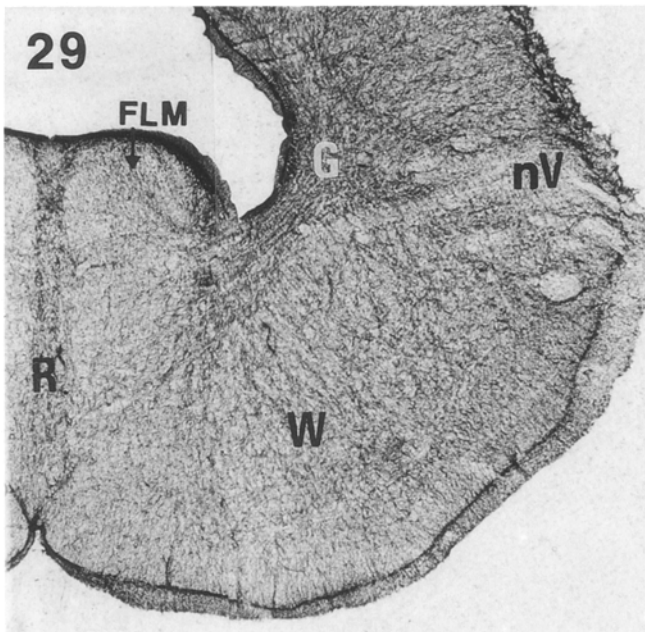
Fig. 29. Pons. G, Gray matter; W, white matter (with higher magnification the pattern is similar to that shown in Fig. 21); R, raphe;

FLM, medial longitudinal fascicle; nV, trigeminal nerve. The open part of the medulla has a similar distribution of GFAP-immunopositivity. × 20

Fig. 30. Spinal cord. G,W, gray and white matter. × 30

Fig. 31. Enlarged part of the white matter. Note the glial septa dividing the white matter into bundles. × 150

32

33

34

35
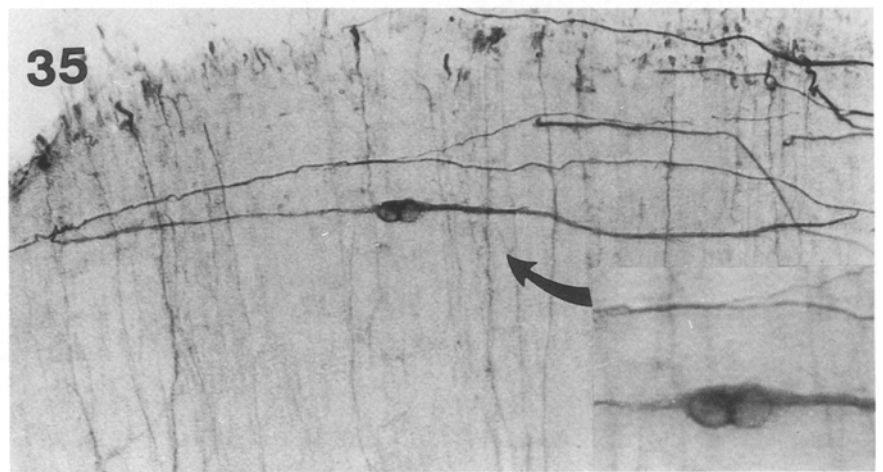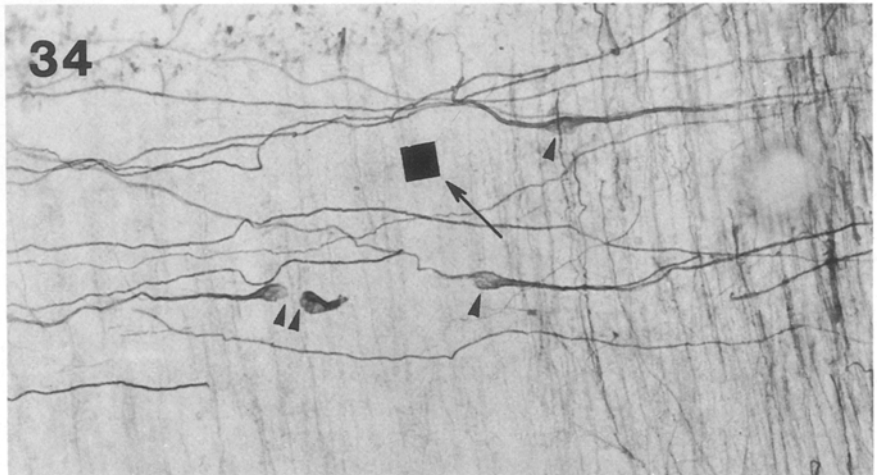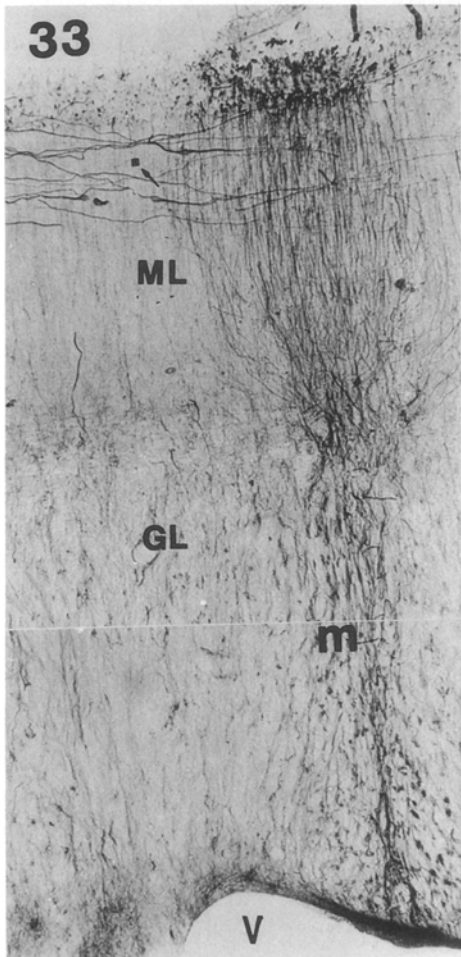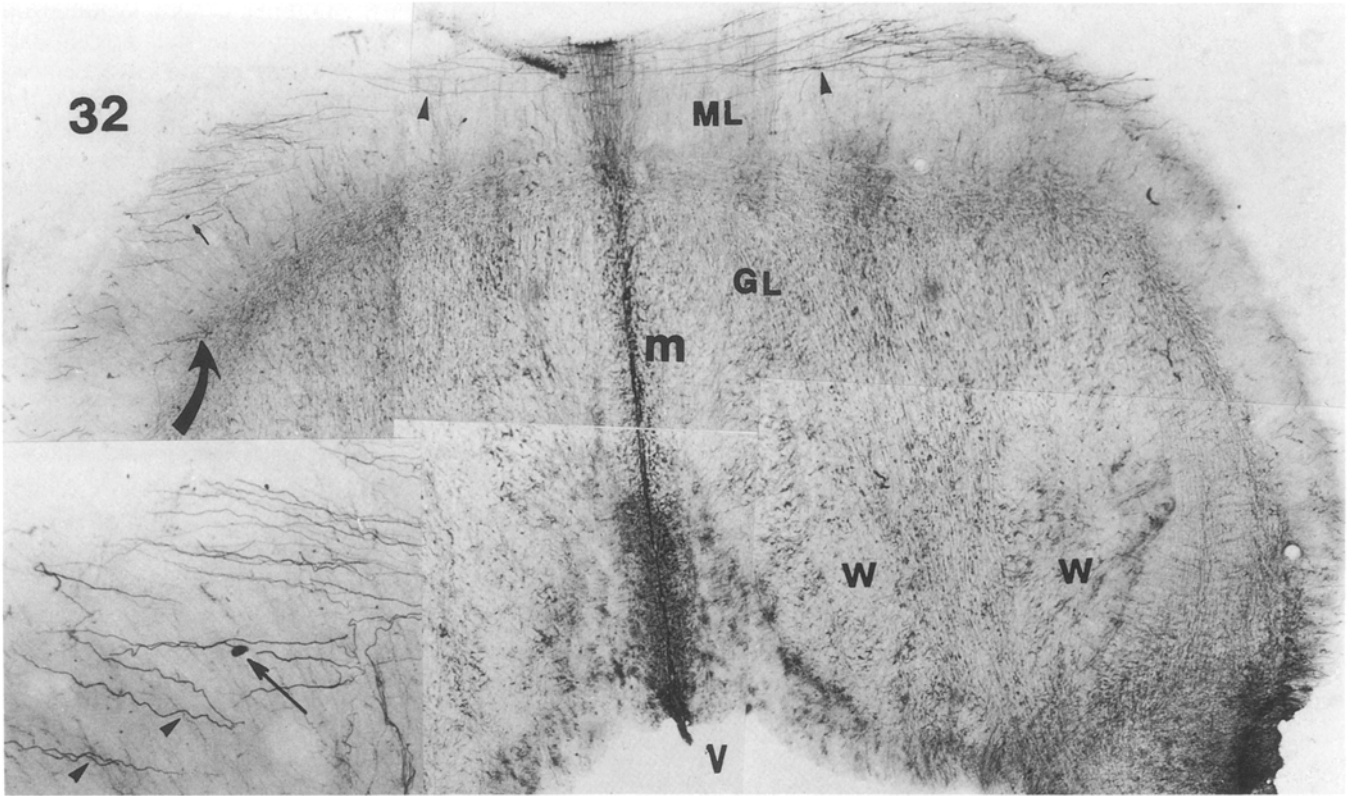
growth (for reviews, see Joosten and Gribnau 1989; Silver et al. 1982; Valentino et al. 1983) or is a secondary phenomenon, needs further investigations.

The optic tectum may be the best example of the principal difference between the types of GFAP-immunostaining in the avian and chelonian brains. The tectum consists of the same layers in both turtles and birds (Kuenzel and Masson 1988; Powers and Reiner 1980). In the chicken, however, a dense system of radial fibers can be found only during the early post-hatching period (Kálmán et al. 1993b) but not in adults (Kálmán et al. 1993a; Linser 1985). Although evenly distributed astrocytes can be demonstrated by glutamine synthetase immunostaining in all layers, GFAP-immunopositive cells can be found only in the deeper layers (Kálmán et al. 1993a; Linser 1985).

The distinction between gray and white matter that can be observed in the spinal cord of mammals and birds after GFAP-immunostaining can be followed in the turtle brain stem up to the posterior part of the diencephalon, probably because of the less complicated organization of the reticular formation.

It has been suggested that in the molecular layer of the cerebellum the abundant system of fine GFAP-positive fibers corresponds to the Bergmann-fibers of higher Vertebrates. The observation that these fibers are not attenuated continuations or finer branches of the coarser fibers of the granular layer, but seem to originate at the border of the molecular and granular layers, is also consistent with this opinion (Dahl et al. 1985).

The pony-tail pattern of GFAP-positive fibers in the midline of the cerebellum resembles the raphe glial structures observed in the developing rat and chicken brain stem (Kálmán et al. 1989; 1993b), indicating that the development of the cerebellum in the lower vertebrates is still rather similar to that of the other thickened parts of the brain stem.

The formation and function of the transverse fibers of the molecular layer of the cerebellum needs further investigation. No similar structure has ever been observed in the cerebellum of mammals (Bignami and Dahl 1974; Hajós and Kálmán 1989; Kótai et al. 1989; Schachner

et al. 1977) birds (Kálmán et al. 1993a; Roeling and Feirabend 1988), amphibians (Korte and Rosenbluth 1981) or fish (Kálmán 1993). The studies published by Monzon-Mayor et al. (1990) and Yanes et al. (1990) on the lizard brain, and the Golgi studies reported by Stensaans and Stensaans (1968) on the turtle brain did not include the cerebellum.

In conclusion, we suggest that it was the appearance of stellate GFAP-positive cells that made possible further evolution in the directions of both the "conservative" avian brain, which preserved many reptilian features) and the "reformer" mammalian brain, which acquired new telencephalic structures). The stellate cells (astrocytes) can form a more economical glial network and promote: (1) thickening of the brain wall and (2) local differences of GFAP-content.

In a stellate cell, the average distance between the nucleus and other cell parts and the surface/volume ratio are less than in a cell with one elongated fiber. The increasingly disadvantageous conditions for ion-equilibrium limit the length of radial fibers in higher vertebrates and stimulate their division and transformation into stellate cells (Eberhardt and Reichenbach 1987). The individual astrocytes can show rather different GFAP-immunoreactivity (Connor and Berkowitz 1985; Hajós and Kálmán 1989; Linser 1985; Ludwin et al. 1976; Patel et al. 1985) with the result that the different GFAP content of different brain areas can be adapted to the structural and functional features of the local neuronal systems.

References

Alvarez-Buylla A, Theelen M, Nottebohm F (1990) Proliferation "hot spots" in adult avian ventricular zone reveal radial cell division. Neuron 5:101–109

Ariëns Kappers CU, Huber CG, Crosby EC (1960) The comparative anatomy of the nervous system of vertebrates, including man. Hafner, New York

Bignami A, Dahl D (1974) The development of Bergmann glia in mutant mice with cerebellar malformations: reeler, staggerer and weaver. Immunofluorescence study with antibodies to the glial fibrillary acidic protein. J Comp Neurol 155:219–230

Connor JR, Berkowitz RM (1985) A demonstration of glial filament distribution in astrocytes isolated from rat cerebral cortex. Neuroscience 16:33–44

Connors BW, Kriegstein AR (1986) Cellular physiology of the turtle visual cortex: distinctive properties of pyramidal and stellate neurons. J Neurosci 6:167–177

Dahl D, Bignami A (1973) Immunohistochemical and immunofluorescence studies of the glial fibrillary acidic protein in vertebrates. Brain Res 61:279–293

Dahl D, Crosby CJ, Sethi J, Bignami A (1985) Glial fibrillary acidic (GFA) protein in vertebrates: immunofluorescence and immunoblotting study with monoclonal and polyclonal antibodies. J Comp Neurol 239:75–88

Davydova TV, Goncharova NV (1979) Comparative characterization of the basic forebrain cortical zones in *Emys orbicularis* (Linneaus) and *Testudo horsfieldi* (Gray). J Hirnforsch 20:245–265

Fig. 32. Overview of cerebellum × 20. *V,* Ventricle; *m,* midline fiber system; *ML,GL,* molecular and granular layers; *W,* area of GFAP-pattern resembling white matter tracts; *arrowheads,* transverse fibers; *black dot* pointed out by *arrow,* the position of the area enlarged in the inset *(curved arrow),* which shows the angle of the interception of the perpendicular and transverse fibers *(arrowheads)* in the lateral part of molecular layer. × 100

Fig. 33. The midline fiber system, caudally from the section shown in Fig. 32. Abbreviations as in Fig. 32. Note the differences between the fiber patterns of the granular and molecular layers. *Black rectangle* pointed out by *arrow* shows the area enlarged in Fig. 34. × 90

Fig. 34. Enlarged part of Fig. 33 around the rectangle. Note the GFAP-positive perikarya with two transverse fibers *(arrowheads)* and the pair of perikarya with one process each pointing in opposite directions *(double arrowheads)*

Fig. 35. A perikaryon with two immunonegative spaces for nuclei × 250. See this enlarged in the *inset (curved arrow).* × 500

Debus E, Weber K, Osborn M (1983) Monoclonal antibodies specific for glial fibrillary acidic (GFA) protein and for each of the neurofilament triplet polypeptides. Differentation 25:193–203

Eberhardt W, Reichenbach A (1987) Spatial buffering of potassium by retinal Müller (glial) cells of various morphologies calculated by a model. Neuroscience 36:121–144

Hajós F, Bascó E (1984) The surface contact glia. Adv Anat Embryol Cell Biol 84:1–81

Hajós F, Kálmán M (1989) Distribution of glial fibrillary acidic protein (GFAP)-immunoreactive astrocytes in the rat brain. II. Mesencephalon, rhombencephalon and spinal cord. Exp Brain Res 78:164–173

Joosten EAJ, Gribnau AAM (1989) Astrocytes and guidance of outgrowing corticospinal tract axons in the rat. An immunocytochemical study using anti-vimentin and anti-glial fibrillary acidic protein. Neuroscience 31:439–452

Kálmán M (1993) Vimentin persists in the mature glia of fish brain Neurobiology 1:47–54

Kálmán M, Hajós F (1989) Distribution of glial fibrillary acidic protein (GFAP)-immunoreactive astrocytes in the rat brain. I. Forebrain. Exp Brain Res 78:147–163

Kálmán M, Korpás DI, Török C (1989) GFAP-immunopositivity in developing rat brain. Eur J Neurosci [Suppl 2]:47

Kálmán M, Székely A, Csillag A (1993a) Distribution of glial fibrillary acidic protein-immunopositive structures in the brain of the domestic chicken (Gallus domesticus). J Comp Neurol 330:221–237

Kálmán M, Székely A, Csillag A (1993b) GFAP and vimentin in the developing chicken brain. Anat Anz [Suppl 175]:130–131

Korte GE, Rosenbluth J (1981) Ependymal astrocytes in frog cerebellum. Anat Rec 199:267–279

Kótai I, Hajós F, Seress L (1989) Comparative study of glial fibrillary acidic protein (GFAP)-immunoreactivity in the rat and monkey cerebellum. Acta Morphol Hung 37:85–92

Kriegstein AR, Shen JM, Eshhar N (1986) Monoclonal antibodies to the turtle cortex reveal neuronal subsets, antigenic cross-reactivity with the mammalian neocortex, and forebrain structures sharing a pallial derivation. J Comp Neurol 254:330–340

Kuenzel WJ, Masson M (1988) A stereotaxic atlas of the brain of the chick (Gallus domesticus). The Johns Hopkins University Press, Baltimore

Linser PJ (1985) Multiple marker analysis in the avian optic tectum reveals three classes of neuroglia and carbonic anhydrase-containing neurons. J Neurosci 5:2388–2396

Ludwin SK, Kosek JC, Eng LF (1976) The topographical distribution of S-100 and GFA proteins in the adult rat brain: an immunocytochemical study using horseradish peroxidase-labelled antibodies. J Comp Neurol 165:197–208

Monzon-Mayor M, Yanes C, Tholey G, Barry J de, Gombos G (1990) Glial fibrillary acidic protein and vimentin immunohistochemistry in the developing and adult midbrain of the lizard Gallotia galloti. J Comp Neurol 295:569–579

Onteniente B, Kimura H, Maeda T (1983) Comparative study of the glial fibrillary acidic protein in vertebrates by PAP immunohistochemistry. J Comp Neurol 215:427–436

Patel AJ, Weir MO, Hunt A, Tahourdin CSM, Thomas DGT (1985) Distribution of glutamine synthetase and glial fibrillary acidic protein and correlation with glutamate decarboxylase in different regions of the rat central nervous system. Brain Res 331:1–9

Powers AS, Reiner A (1980) A stereotaxic atlas of the forebrain and midbrain of the eastern painted turtle (Chrysemys picta picta). J Hirnforsch 21:125–159

Rakic P (1981) Neuronal-glial interaction during development. Trends Neurosci 4:184–187

Reiner A (1991) A comparison of neurotransmitter-specific and neuropeptide-specific neuronal cell types present in the dorsal cortex in turtles with those present in the isocortex of mammals: implications for the evolution of isocortex. Brain Behav Evol 38:53–91

Riss W, Halpern M, Scalia F (1969) The quest for clues to forebrain evolution – the study of reptiles. Brain Behav Evol 2:1–50

Roeling TAP, Feirabend HKP (1988) Glial fiber pattern in the developing chicken cerebellum: vimentin and glial fibrillary acidic protein (GFAP) immunostaining. Glia 1:398–402

Romer AS (1959) Ther vertebrate story. University of Chicago Press, Chicago

Romer AS (1972) The vertebrate body. Saunders, Philadelphia

Schachner M, Hedley-White ET, Hsu DW, Schoonmaker G, Bignami A (1977) Ultrastructural localization of glial fibrillary acidic protein in mouse cerebellum by immunoperoxidase labelling. J Cell Biol 75:67–73

Silver J, Lorenz SE, Wahlstein D, Coughlin J (1982) Axonal guidance during development of the great cerebral commissures: descriptive and experimental studies in vivo on the role of preformed glial pathways. J Comp Neurol 210:10–29

Stensaans LJ, Stensaans SS (1968) Light microscopy of glial cells in turtles and birds. Z Zellforsch Mikrosk Anat 91:315–340

Valentino KL, Jones EG, Kane SA (1983) Expression of GFAP immunoreactivity during development of long fiber tracts in the rat CNS. Dev Brain Res 9:317–336

Yanes C, Monzon-Mayor M, Ghandour MS, Barry J de, Gombos G (1990) Radial glia and astrocytes in developing and adult telencephalon of the lizard Gallotia galloti as revealed by immunohistochemistry with anti-GFAP and anti-vimentin antibodies. J Comp Neurol 295:559–568

Zilles K, Hajós F, Kálmán M, Schleicher A (1991) Mapping of glial fibrillary acidic protein immunoreactivity in the rat forebrain and mesencephalon by computerized image analysis. J Comp Neurol 308:340–355